A Unified View of Ethylene Polymerization by d^0 and d^0f^n Transition Metals. 1. Precursor Compounds and Olefin Uptake Energetics

Peter Margl, Liqun Deng, and Tom Ziegler*

Department of Chemistry, University of Calgary, 2500 University Drive, N.W., T2N 1N4 Calgary, Alberta, Canada

Received August 25, 1997

A systematic study has been carried out on the complexation of ethylene to a number of d^0 $[L]MC_2H_5^{0,+,2+}$ fragments [M = Sc(III), Y(III), La(III), Lu(III), Ti(IV), Zr(IV), Hf(IV), Ce(IV), Th(IV), and V(V); L = $NH(CH)_2NH^{2-}$ (**1**), $N(BH_2)(CH)_2(BH_2)N^{2-}$ (**2**), $O(CH)_3O^-$ (**3**), Cp_2^{2-} (**4**), $NHSi(H_2)C_5H_4^{2-}$ (**5**), $[(oxo)(O(CH)_3O)]^{3-}$ (**6**), $(NH_2)_2^{2-}$ (**7**), $(OH)_2^{2-}$ (**8**), $(CH_3)_2^{2-}$ (**9**), and $NH(CH_2)_3NH^{2-}$ (**10**)], where a hydrogen on the β-carbon of the ethyl unit is bound to the metal in an agostic interaction (β-agostic bond). It is shown that the complexation energy of an ethylene molecule to a $[L]MC_2H_5^{n+}$ precursor can be predicted to within ±20 kJ/mol by simple empirical rules, based on the accessible metal surface of the $[L]MC_2H_5^{n+}$ fragment and its gross charge. Discussions are also given of the relative preference for frontside (ethylene syn to β-agostic bond) versus backside (ethylene anti to β-agostic bond) coordination by the olefin as a function of the central atom, the auxiliary ligand set L and the strength of the β-agostic bond. It is finally shown that the β-agostic bond strength in the $[L]MC_2H_5^{n+}$ precursor follows the order Ti ≈ Zr > Th > Hf for $[L]MC_2H_5^+$ and Sc ≈ Y ≥ La > Lu for $[L]MC_2H_5$ for L = **7**−**9**, with agostic interactions for uncharged precursor complexes $[L]MC_2H_5$ generally being weaker than for charged precursor complexes.

Introduction

Single-site olefin polymerization catalysts composed of a group 4 metallocene complex have been developed to a high degree of sophistication over the past decade as alternatives to the classical Ziegler−Natta catalysts comprised of titanium halides and alkylaluminum.[1] Most recently the search for single-site catalysts has been extended beyond group 4 metallocenes in the hope of achieving superior polymer specifications and lower production costs.[2−6] For example, Brookhart and coworkers have developed diimine Ni- and Pd-based d^8 systems which give branched polymers with highly desirable strength and processing properties.[7−9] Progress has also been made for d^0 systems, involving mostly amido, amino, or alkoxide ligands plus combinations thereof with the cyclopentadienyl ligand motif coordinated to Ti(IV), Zr(IV), and Hf(IV) centers.[3,4,10−25] It has been claimed that some of the latter metal−ligand combinations are active as olefin polymerization catalysts,[10−12,14,18,19,21] whereas some have been reported to be inferior in this regard.[15−17,20] Different behaviors encountered for d^0 type complexes are often attributed to electronic influences of the ligand.[26] However, the reasons for different performances of d^0 complexes are not yet fully understood.

(1) Brintzinger, H. H.; Fischer, D.; Mülhaupt, R.; Rieger, B.; Waymouth, R. M. *Angew. Chem., Int. Ed. Engl.* **1995**, *34*, 1143.
(2) Pellecchia, C.; Zambelli, A. *Macromol. Rapid Commun.* **1996**, *17*, 333.
(3) Antonelli, D. M.; Leins, A.; Stryker, J. M. *Organometallics* **1997**, *16*, 2500.
(4) Murphy, V. J.; Turner, H. *Organometallics* **1997**, *16*, 2495.
(5) White, P. A.; Calabrese, J.; Theopold, K. H. *Organometallics* **1996**, *15*, 5473.
(6) Liang, Y.; Yap, G. P. A.; Rheingold, A. L.; Theopold, K. H. *Organometallics* **1996**, *15*, 5284.
(7) Johnson, L. K.; Killian, C. M.; Brookhart, M. *J. Am. Chem. Soc.* **1995**, *117*, 6414.
(8) Johnson, L. K.; Mecking, S.; Brookhart, M. *J. Am. Chem. Soc.* **1996**, *118*, 267.
(9) Killian, C. M.; Tempel, D. J.; Johnson, L. K.; Brookhart, M. *J. Am. Chem. Soc.* **1996**, *118*, 11664.
(10) Scollard, J. D.; McConville, D. H. *J. Am. Chem. Soc.* **1996**, *118*, 10008.
(11) Scollard, J. D.; McConville, D. H.; Payne, N. C.; Vittal, J. J. *Macromolecules* **1996**, *29*, 5241.
(12) Shah, S. A. A.; Dorn, H.; Voigt, A.; Roesky, H.; Parisini, E.; Schmidt, H.-G.; Noltemeyer, M. *Organometallics* **1996**, *15*, 3176.
(13) Fokken, S.; Spaniol, T. P.; Kang, H.-C.; Massa, W.; Okuda, J. *Organometallics* **1996**, *15*, 5069.
(14) van der Linden, A.; Schaverien, C. J.; Meijboom, N.; Ganter, C.; Orpen, A. G. *J. Am. Chem. Soc.* **1995**, *117*, 3008.
(15) Warren, T. H.; Schrock, R. R.; Davis, W. M. *Organometallics* **1996**, *15*, 562.
(16) Brand, H.; Capriotti, J. A.; Arnold, J. *Organometallics* **1994**, *13*, 4469.
(17) Tjaden, E. B.; Swenson, D. C.; Jordan, R. F.; Petersen, J. L. *Organometallics* **1995**, *14*, 371.
(18) Horton, A. D.; de With, J.; van der Linden, A. J.; van de Weg, H. *Organometallics* **1996**, *15*, 2672.
(19) Fuhrmann, H.; Brenner, S.; Arndt, P.; Kempe, R. *Inorg. Chem.* **1996**, *35*, 6742.
(20) Cozzi, P. G.; Gallo, E.; Floriani, C.; Chiesi-Villa, A.; Rizzoli, C. *Organometallics* **1995**, *14*, 4994.
(21) Cloke, F. G. N.; Geldbach, T. J.; Hitchcock, P. B.; Love, J. B. *J. Organomet. Chem.* **1996**, *506*, 343.
(22) Uhrhammer, R.; Black, D. G.; Gandner, T. G.; Olsen, J. D.; Jordan, R. F. *J. Am. Chem. Soc.* **1993**, *115*, 8493.
(23) Long, D. P.; Bianconi, P. A. *J. Am. Chem. Soc.* **1996**, *118*, 12453.
(24) Aoyagi, K.; Gantzel, P. K.; Kalai, K.; Tilley, T. D. *Organometallics* **1996**, *15*, 923.
(25) Jia, L.; Yang, X.; Stern, C.; Marks, T. J. *Organometallics* **1994**, *13*, 3755.
(26) Richardson, D. E.; Alameddin, G. A.; Ryan, M. F.; Hayes, T.; Eyler, J. R.; Siedle, A. R. *J. Am. Chem. Soc.* **1996**, *118*, 11244.

S0276-7333(97)00757-7 CCC: $15.00
Publication on Web 02/12/1998

Scheme 1

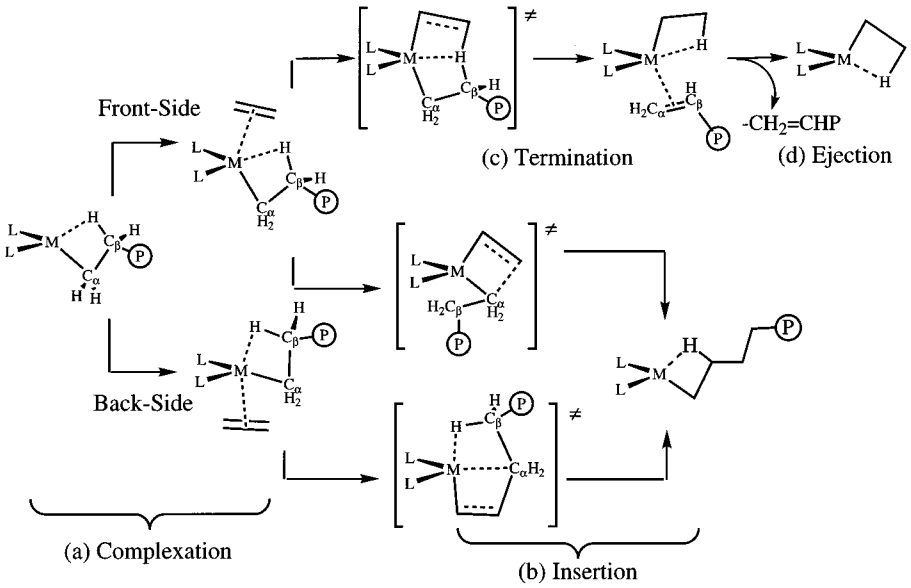

In the present series of papers, we aim at an understanding of the generic olefin insertion process and how it is affected by change of metal and ligand in terms of high-level first principles calculations. We restrict ourselves to d^0 complexes, in the hope of being able to generalize our findings to higher d-occupations.

It is widely accepted that the efficiency of a polymerization catalyst depends on a great variety of factors, some of which are not even related to the catalyst itself but to a counterion or a solvent.[10,11,27] However, it is a necessary condition for a working catalyst to have a high intrinsic aptitude toward the so-called "chain propagation" step and a low aptitude toward all competing "chain termination" processes. As shown in Scheme 1, the chain propagation process for Ziegler type catalysts is initiated by (a) olefin uptake followed by (b) an insertion reaction between the metal−polymer bond and the incoming olefin. The often dominant competing process is transfer of a polymer β-hydrogen atom to the approaching olefin (c), leading to termination of the chain and regrowth of a new chain, after the terminated chain has been ejected (d). As a first step toward our ultimate aim of systematically evaluating the intrinsic aptitude of various d^0 metals to polymerize olefins, we describe step (a) of the cycle, the olefin binding energetics for d^0 and d^0f^n metal centers. Since uptake and ejection processes a and d are virtually identical apart from the fact that ejection involves a longer substituent (P in Scheme 1) on the olefin, our results also pertain to the ejection process d.

The size of the binding energy of an olefin to the metal center can influence the course of the polymerization reaction in a number of ways: (a) The binding enthalpy, ΔH, from the complexation of olefin to the catalyst should be sufficiently exothermic ($-\Delta H > 40$ kJ/mol) to make the corresponding free energy of complexation, $\Delta G = \Delta H - T\Delta S$, negative despite a large negative entropy of complexation, ΔS, that occurs if the ethylene is complexed to a metal center. If this is not the case, catalytic activity might be negligible even if the insertion barrier $\Delta H^{\neq}$ on the potential energy surface is very low. Additionally, a positive ΔG can also lead to very low molecular weights since in the absence of a sufficiently stable π-complex, first-order termination mechanisms such as β-hydrogen transfer to the metal will eventually be weight-determining although they may be negligible in cases where a more stable π-complex can be formed.[28] (b) Stereochemical properties are also determined by the manner of π-complexation, since stereoregularity is often effected by a preference for a given insertion pathway as discussed by Bierwagen et al.[29] and Lohrenz et al.[30] (c) If a vinyl-terminated chain cannot be ejected due to a high binding energy, regrowth of a new chain might be disfavored compared to chain branching since the terminated chain will be reinserted immediately.

As a representative sample of d^0 metal centers, we chose Sc(III), Y(III), La(III), Lu(III), Ti(IV), Zr(IV), Hf(IV), Ce(IV), Th(IV), and V(V). A sample of ligands was constructed to reflect trends in the recent experimental literature, which has focused mostly on nitrogen- and oxygen-based ligands.[12,14,16−22] Therefore we chose 10 ligands (L = $NH(CH)_2NH^{2-}$ (**1**), $N(BH_2)(CH)_2(BH_2)N^{2-}$ (**2**), $O(CH)_3O^-$ (**3**), Cp_2^{2-} (**4**), $NHSi(H_2)C_5H_4^{2-}$ (**5**), $[(O)(O(CH)_3O)]^{3-}$ (**6**), $(NH_2)_2^{2-}$ (**7**), $(OH)_2^{2-}$ (**8**), $(CH_3)_2^{2-}$ (**9**), and $NH(CH_2)_3NH^{2-}$ (**10**), Scheme 2) to represent most current trends in experimental work.[31] Whereas experimentally studied catalysts often have large substituents on the coligands, we do explicitly not consider steric hindrance deriving from large substituents (except when those ligands form an irreducible entity, for instance $(Cp)_2$) since it is our aim to outline the influence

(27) Chen, Y.-X.; Stern, C. L.; Yang, S.; Marks, T. J. *J. Am. Chem. Soc.* **1996**, *118*, 12451.

(28) Woo, T. K.; Margl, P.; Ziegler, T.; Blöchl, P. E. *Organometallics* **1997**, *16*, 3454.

(29) Bierwagen, E. B.; Bercaw, J. E.; Goddard,W. A., III. *J. Am. Chem. Soc.* **1994**, *116*, 1481.

(30) Lohrenz, J. C. W.; Woo, T. K.; Ziegler, T. *J. Am. Chem. Soc.* **1995**, *117*, 12793.

(31) Some of the calculations discussed here were done and analyzed in other publications ([**5**]Ti,[32] [**4**]Zr,[30] and [**10**]M (M = Ti, Zr, Hf)[48]) based on the same density functional approach. They are not repeated here but simply referred to as literature data. Geometries pertaining to these calculations are also not included in the Supporting Information.

Scheme 2

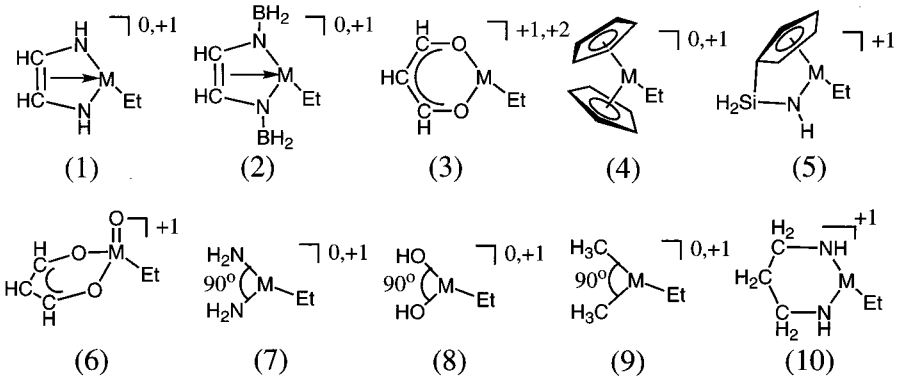

of the metal and the first coordination sphere on olefin complexation and insertion energetics.

We use an ethyl group as a model for the growing polymer chain, since methyl on one hand cannot reproduce the β-agostic bonding situation which is the direct precursor of olefin insertion. Longer chains, on the other hand, drastically increase computation time without adding crucial information since γ- and higher agostic bonds are usually replaced by β-agostic ones prior to insertion, as shown by Woo et al.[32] In the present work, we confine ourselves to the olefin uptake reaction, whereas subsequent papers will describe the insertion and termination reactions.

Computational Details

Stationary points on the potential energy surface were calculated with the program ADF, developed by Baerends et al.[33,34] and vectorized by Ravenek.[35] The numerical integration scheme applied for the calculations was developed by te Velde et al.[36,37] The geometry optimization procedure was based on the method due to Versluis[38] and Ziegler. The frozen core approximation was employed throughout. The electronic configurations of the molecular systems were described by a triple-ζ Slater type basis set on metal atoms and by a double-ζ quality basis on nonmetal atoms (Table 1).[39,40] A set of auxiliary[41] s, p, d, f, and g STO functions, centered on all nuclei, was used in order to fit the molecular density and present Coulomb and exchange potentials accurately in each SCF cycle. Energy differences were calculated by augmenting the local exchange-correlation potential by Vosko et al.[42] with Becke's[43] nonlocal exchange corrections and Perdew's[44,45] nonlocal correlation correction. Geometries were optimized including nonlocal corrections. First-order scalar relativistic corrections[46,47] were added to the total energy for all systems containing 3d and 4d metal atoms, since a perturbative relativistic approach is sufficient for those as shown by Deng.[48] On all systems containing either lanthanide, actinide, or 5d metal atoms, quasi-relativistic geometry optimizations were carried out.[49] In cases where the stability of a stationary point appeared doubtful, several geometry optimizations were done starting from different initial geometries. In view of the fact that all systems investigated in this work show a large HOMO−LUMO gap, a spin-restricted formalism was used for all calculations. No symmetry constraints were used except where explicitly indicated. In a number of previous papers, transition metal−ligand dissociation energetics have been proven to be correct within 5 kcal/mol of the experimental result,[50−53] usually overestimated in terms of absolute size.

Table 1. Frozen Cores and Slater Type Basis Functions for All Atoms Used in This Study

	frozen core	valence basis set[a]	polarization
H		1s dζ	2p sζ
B	[He]	2s 2p dζ	3d sζ
C	[He]	2s 2p dζ	3d sζ
N	[He]	2s 2p dζ	3d sζ
O	[He]	2s 2p dζ	3d sζ
Sc	[Ne]	3s 3p dζ; 3d 4s tζ	4p sζ
Ti	[Ne]	3s 3p dζ; 3d 4s tζ	4p sζ
V	[Ne]	3s 3p dζ; 3d 4s tζ	4p sζ
Y	[Ar]3d^{10}	4s dζ; 4p 4d 5s tζ	5p sζ
Zr	[Ar]3d^{10}	4s dζ; 4p 4d 5s tζ	5p sζ
Nb	[Ar]3d^{10}	4s dζ; 4p 4d 5s tζ	5p sζ
La	[Xe]	6s 5d 4f tζ	6p sζ
Ce	[Kr]4d^{10}	5s 5p dζ; 4f 5d 6s tζ	6p sζ
Lu	[Xe]	6s 5d 4f tζ	6p sζ
Hf	[Xe]4f^{14}	5d 6s tζ	6p sζ
Th	[Xe]5d^{10}4f^{14}	6s 6p 7s dζ; 5f 6d tζ	7p sζ

[a] sζ = single zeta; dζ = double zeta; tζ = triple zeta.

Results and Discussions

General Considerations. In the following, we outline the results of our DFT calculations and describe

(32) Woo, T.; Margl, P. M.; Lohrenz, J. C. W.; Blöchl, P. E.; Ziegler, T. *J. Am. Chem. Soc.* **1996**, *118*, 13021.
(33) Baerends, E. J.; Ellis, D. E.; Ros, P. *Chem. Phys.* **1973**, *2*, 41.
(34) Baerends, E. J.; Ros, P. *Chem. Phys.* **1973**, *2*, 52.
(35) Ravenek, W. In *Algorithms and Applications on Vector and Parallel Computers*; te Riele, H. J. J., Dekker, T. J., van de Horst, H. A., Eds.; Elsevier: Amsterdam, The Netherlands, 1987.
(36) te Velde, G.; Baerends, E. J. *J. Comput. Chem.* **1992**, *99*, 84.
(37) Boerrigter, P. M.; te Velde, G.; Baerends, E. J. *Int. J. Quantum Chem.* **1988**, *33*, 87.
(38) Versluis, L.; Ziegler, T. *J. Chem. Phys.* **1988**, *88*, 322.
(39) Snijders, J. G.; Baerends, E. J.; Vernoijs, P. *At. Nucl. Data Tables* **1982**, *26*, 483.
(40) Vernoijs, P.; Snijders, J. G.; Baerends, E. J. *Slater Type Basis Functions for the Whole Periodic System*; Internal report (in Dutch); Department of Theoretical Chemistry, Free University, Amsterdam, The Netherlands, 1981.
(41) Krijn, J.; Baerends, E. J. *Fit Functions in the HFS Method*; Internal Report (in Dutch); Department of Theoretical Chemistry, Free University, Amsterdam, The Netherlands, 1984.
(42) Vosko, S. H.; Wilk, L.; Nusair, M. *Can. J. Phys.* **1980**, *58*, 1200.
(43) Becke, A. *Phys. Rev. A* **1988**, *38*, 3098.
(44) Perdew, J. P. *Phys. Rev. B* **1986**, *34*, 7406.
(45) Perdew, J. P. *Phys. Rev. B* **1986**, *33*, 8822.
(46) Snijders, J. G.; Baerends, E. J. *Mol. Phys.* **1978**, *36*, 1789.
(47) Snijders, J. G.; Baerends, E. J.; Ros, P. *Mol. Phys.* **1979**, *38*, 1909.
(48) Deng, L.; Ziegler, T. *J. Am. Chem. Soc.*, submitted for publication.
(49) Ziegler, T.; Tschinke, V.; Baerends, E. J.; Snijders, J. G.; Ravenek, W. *J. Phys. Chem.* **1989**, *93*, 3050.
(50) Folga, E.; Ziegler, T. *J. Am. Chem. Soc.* **1993**, *115*, 5169.
(51) Li, J.; Schreckenbach, G.; Ziegler, T. *J. Phys. Chem.* **1994**, *98*, 4838.
(52) Li, J.; Schreckenbach, G.; Ziegler, T. *J. Am. Chem. Soc.* **1995**, *117*, 486.
(53) Li, J.; Schreckenbach, G.; Ziegler, T. *Inorg. Chem.* **1995**, *34*, 3245.

Scheme 3

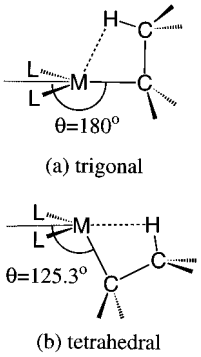

in detail the factors responsible for the systematic trends in the calculated ethylene π-complex formation energies. Since it is not possible to give a detailed discussion of all geometries involved, we restrain ourselves to verbally describing important geometric features and refer to Supporting Information for more detail.

For clarity we repeat here some fundamental facts about the type of d^0 complexes under investigation. Scheme 3 shows that given a typical arrangement of ligands where two coordination sites are occupied by the auxiliary ligand set [L], the growing chain (in this case ethyl) occupies the remaining coordination sites with the M−C_α bond and typically one or two agostic bonds, where C−H linkages are bound to the metal center through hydrogen. The β-agostic bond involving hydrogens on the β-carbon is usually strongest. If more than two coordination sites are occupied by an auxiliary ligand, agostic interactions decrease in strength due to steric congestion. In previous work, it was observed that an incoming olefin forms a π-complex prior to insertion. Complex formation can occur syn or anti to an already existing β-agostic bond. As in previous publications, we will term the resulting complexes the frontside (FS) and backside (BS) complex,[28,30,32] respectively (Scheme 1).

(1) Geometries and Energetics of the Precursor Fragments [L]$MC_2H_5^{n+}$ (n = 0, 1, 2). Compounds of the composition [L]MR^{n+} are supposed to be the precursors for olefin complexation and subsequent chain propagation (Scheme 1). As shown in Scheme 3, there are two limiting structures for [L]MR^{n+}. The first, the trigonal conformation (a), has [L] and C_α in a coplanar arrangement and represents the precursor for a BS π-complex. The second, the tetrahedral conformation (b), has [L] and the agostic hydrogen in the same plane, whereas the LMC_α angle is near the tetrahedral value of 109°. It constitutes the precursor for the FS π-complex. We will now in detail investigate the conformational energetics determining the relative stabilities of the tetrahedral and trigonal conformations, which in turn to a large degree will determine the relative stabilities of the FS and BS π-complexes. For the purpose of the following discussion, we will divide the factors which determine the relative stabilities of the two conformations into (a) direct primary ligand interactions from the M−L and M−C_α bonds and (b) indirect secondary ligand interactions represented by agostic bonding.

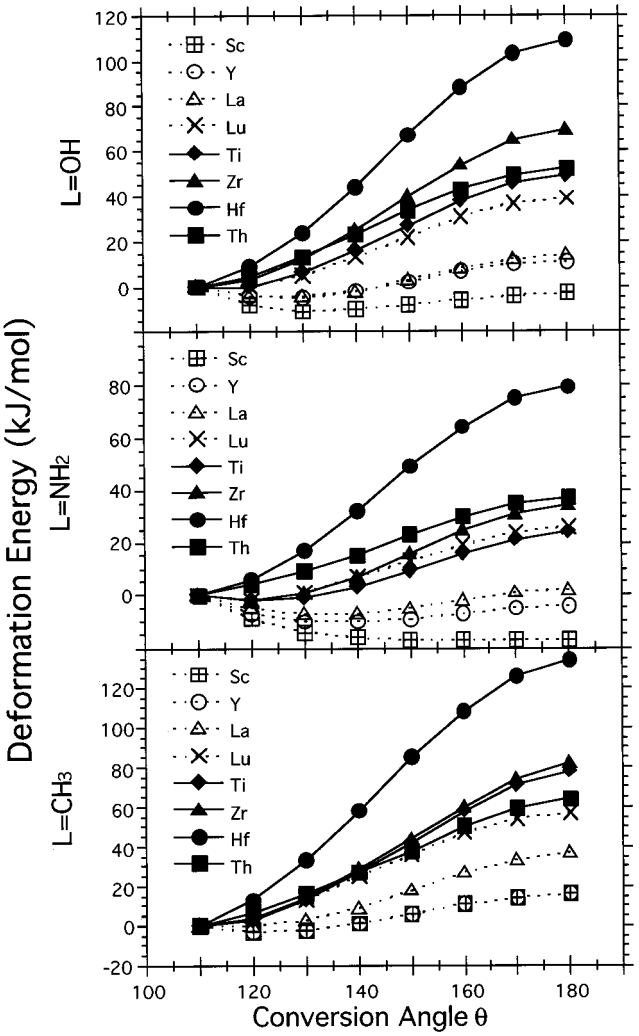

Figure 1. Dependence of the total energy of $L_2MCH_3^{n+}$ on the conversion angle θ, defined as the angle between the L−L centroid, the metal atom, and the α carbon atom. The following constraints were in place: angle L−M−L = 90°; torsion L−X−M−C_α = 90°; angle M−C_α−H_α = 109.45°. X is the L−L centroid; L is either C, N, or O. The M−C_α−H_α angles were constrained to 109.45° in order to avoid α-agostic bonding.

(1.a) Influence of Direct, Primary Ligand Interactions on the Preference for Trigonal vs Tetrahedral Conformation. To approximately separate the two above-mentioned factors, namely relative stability of the metal framework and agostic bonding, we juxtapose two groups of idealized model systems, namely $L_2MCH_3^{n+}$ and $L_2MC_2H_5^{n+}$ (M = Sc, Y, La, Lu, Ti, Zr, Hf, Th; L = CH_3, NH_2, OH). The two ligand groups L are kept at a typical bidentate angle of 90° to each other by means of a constraint but are otherwise free to change.[54] First, we carry out a series of calculations where the interconversion angle θ (see Scheme 3) for $L_2MCH_3^{n+}$ is varied from 110 to 180°, corresponding to a change from tetrahedral to trigonal. *The resulting change in total energy can be considered a good measure of the relative stability of the metal framework if no agostic bonding is present.*

Figure 1 shows that usually the tetrahedral conformation is much preferred over the trigonal conforma-

(54) To preclude any α-agostic bonding, the angles between metal, methyl carbon, and methyl hydrogens were constrained to 109.45°.

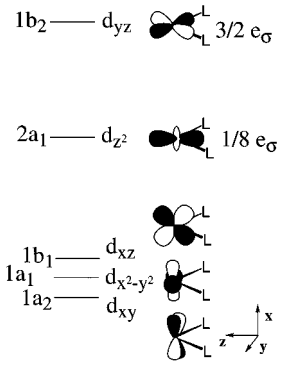

Figure 2. Schematic view of the d orbitals of a L_2M d^0 fragment in C_{2v} symmetry according to the angular overlap method.

tion, with the exception of $(NH_2)_2ScCH_3$. *Irrespective of the ligand, Sc triad metals have a stronger tendency toward trigonal conformation than Ti triad metals. Furthermore, the preference for tetrahedral conformation increases as one moves down in the periodic table.*

Within a triad, the increasing preference for the tetrahedral conformation can be explained by steric and electronic arguments: First, sterics will always favor the trigonal over the tetrahedral conformation, since trigonal arrangement of the ligands minimizes steric conflicts. Therefore, a big metal ion at the bottom of a triad will favor the tetrahedral conformation more than a small metal ion at the top of a triad.

Second, electronic terms also increase the preference of the L_2MR^{n+} species for the tetrahedral conformation toward the bottom of a triad. We can understand this by considering the interaction between R and the L_2M^{n+} fragment (angle LML = 90°) in the two conformations. To this end we provide in Figure 2 the splitting of the d-levels for a C_{2v}-symmetric L_2M^{n+} fragment in terms of the e_σ parameter of the angular overlap method (AOM).[55] In the trigonal conformation the M−R bond is formed by an interaction between the σ-orbital of R and $2a_1$ on ML_2. The $2a_1$ orbital is made up of d_{z^2} on the metal destabilized by $^1/_8$ e_σ from interactions with σ-orbitals on the auxiliary ligands L. In the tetrahedral conformation $1a_1$ ($d_{x^2-y^2}$) and b_1 (d_{xz}) of ML_2 can both interact with the σ-orbital of R.

The two metal orbitals $1a_1$ and b_1 are nonbonding with respect to the auxiliary ligands L and thus better able to stabilize the electron pair in the M−R linkage than $2a_1$. As a result, electronic factors should prefer the tetrahedral conformation. *Furthermore, as one goes down a triad, the splitting term e_σ becomes larger (d_{z^2} rises in energy) and therefore the preference of tetrahedral over trigonal conformation is enhanced.*

Spin-restricted open-shell test calculations on C_{2v}-symmetric fragments of the type $(OH)_2M^{0,+1}$ corroborate this view. The splittings (in eV) between $d_{x^2-y^2}$ ($1a_1$) and d_{z^2} ($2a_1$) are as follows: Sc, 1.09; Y, 1.37; Ti, 0.57; Zr, 1.05; Hf, 1.96 (Table 2). For La the energy of the d_{z^2} orbital cannot be resolved unambiguously since it mixes into a number of orbitals throughout a wide energy range (above the energy range of Table 2). In this case, the main weight of the d_{z^2} admixture lies, however, at least 2 eV above the $d_{x^2-y^2}$ level. In this context it is interesting to note that a nonrelativistic calculation on $(OH)_2HfC_2H_5^+$ yields a much smaller preference for tetrahedral configuration than a relativistic one. Correspondingly, the $d_{x^2-y^2}-d_{z^2}$ gap in $(OH)_2Hf^+$ decreases from 1.96 to 1.04 eV, which confirms that the conformational preference within a triad is determined by the $1a_1-2a_1$ splitting. Along the same lines, it was found by Deng and Ziegler[48] that a nonrelativistic calculation on β-agostic [**10**]$HfC_3H_7^+$ actually reverses the preference from tetrahedral (relativistic) to trigonal (nonrelativistic).

A steric argument cannot be applied to resolve the paradoxical situation that there is more of a preference for the tetrahedral conformation among the small group 4 d^0 ions than the big group 3 d^0 centers (Figures 2 and 3). Bierwagen et al.[29] have given an explanation for the increased preference for a tetrahedral configuration in group 4 cations as opposed to group 3 metals, based on their different s−d splittings. According to them, group 4 cations prefer a tetrahedral conformation because of reduced availability of the $(n + 1)$s orbitals relative to nd orbitals in comparison to group 3 metals. Their argument was based on the fact that Ti^+ adopts a $4s^13d^2$ electronic ground-state configuration whereas Sc has a $4s^23d^1$ configuration.

Table 2. Contributions of Metal Basis Functions to the Lowest Unoccupied Orbitals of $(OH)_2M^{0,+}$ [a]

			trigonal[b]			tetrahedral[c]		
metal	orbital	energy (eV)	s	p_z	d_{z^2}	p_x	$d_{x^2-y^2}$	d_{xz}
Sc	$1a_1$[d]	−3.24	63	10			25[e]	
	$1b_1$	−2.27				18		77
	$2a_1$	−2.15		20	56[e]		14	
	$3a_1$	−1.69	9		20		15	
	$2b_1$	0.45				77		14
Y	$1a_1$[d]	−3.22	73	9			15[e]	
	$1b_1$	−1.89				28		69
	$2a_1$	−1.85	4	23	38[e]		29	
	$3a_1$	−1.15	6		31		41	
	$2b_1$	0.34				68		26
La	$1a_1$[d]	−2.89	72	8			16	
	$1b_1$	−2.08				6		43
	$2a_1$	−2.03			12		20	
	$3a_1$	−1.87			14		12	
	$2b_1$	−1.64						
	$3b_1$	−1.21				24		26
	$4b_1$	0.57				67		22
Ti	$1a_1$[d]	−9.87	17		11		68[e]	
	$1b_1$	−9.47						83
	$2a_1$	−9.30			67[e]		10	
	$3a_1$	−7.55	57	24			10	
	$2b_1$	−4.61				92		
Zr	$1a_1$[d]	−9.01	31		9		56[e]	
	$1b_1$	−8.37				7		81
	$2a_1$	−7.96		7	65[e]		8	
	$3a_1$	−7.13	49	20			22	
	$2b_1$	−4.36				92		
Hf	$1a_1$[d]	−10.1	61		8		30[e]	
	$1b_1$	−8.36				7		81
	$2a_1$	−8.11			60[e]		18	
	$3a_1$	−7.61	22		11		37	
	$2b_1$	−4.4				90		7

[a] Spin-restricted calculations performed in C_{2v} symmetry. The molecular rotation axis was aligned with the z axis, and the OH groups were placed into the yz plane. The O−M−O angle was constrained to 90°. Contributions smaller than 5% and f orbital contributions are omitted for clarity. [b] Orbitals which favor trigonal coordination. [c] Orbitals which favor tetrahedral coordination. [d] Singly occupied molecular orbital (SOMO). [e] Used to compute the AOM e_σ splitting discussed in the text.

(55) Larsen, E.; LaMar, G. N. *J. Chem. Educ.* **1974**, *51*, 633.

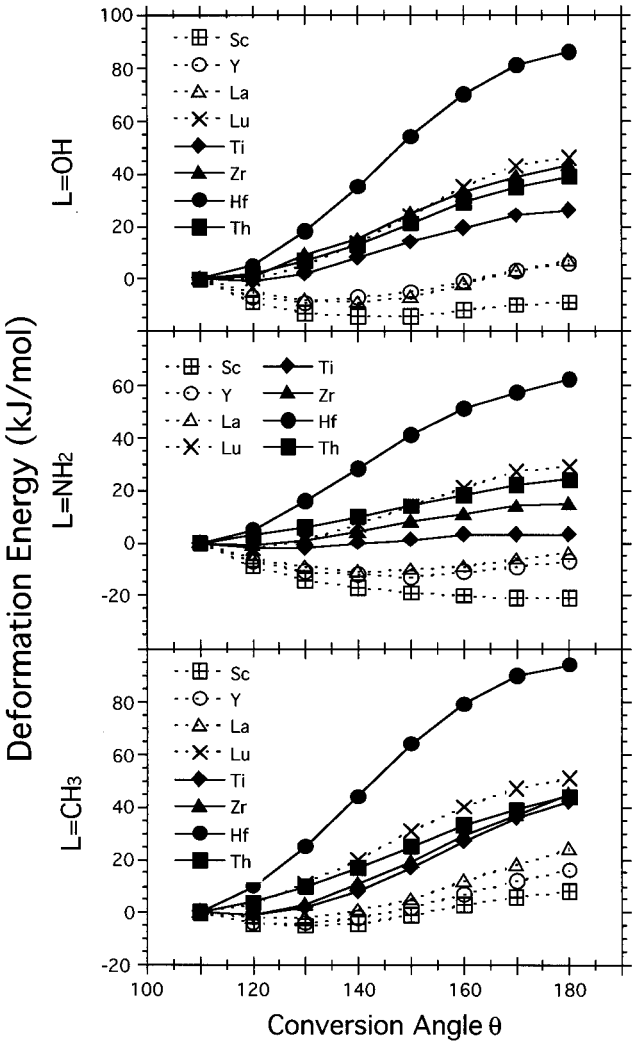

Figure 3. Dependence of the total energy of $L_2MC_2H_5^{n+}$ on the conversion angle θ, defined as the angle between the L−L centroid, the metal atom, and the α carbon atom. The following constraints were in place: angle L−M−L = 90°; torsion L−X−M−C_α = 90°; angle M−C_α−H_α = 109.45°; torsion L−M−C_α−C_β = 180°; torsion M−C_α−C_β−H_β = 0°. X is the L−L centroid. The M−C_α−H_α angles were constrained to facilitate comparison with the methyl calculations.

We afford in Table 2 the composition of the ML_2 frontier orbitals in the case of $(OH)_2M^{0,+1}$ from actual DFT calculations as opposed to the simple AOM treatment of Figure 2. Our calculations show that indeed the $(n + 1)$s orbitals mix into the $1a_1$ (large contribution) and $2a_1$ (small contribution) levels of ML_2 for group 3 metals, whereas $(n + 1)$s participation is less important for group 4 metals. Judging from the SOMO energies in Table 2, it appears that for group 4 metals, metal−alkyl binding will be primarily through d orbitals with *some* s admixture, whereas for group 3 metals, bonding will have a *dominant* contribution from s-type orbitals with a sizable admixture of p_z through the involvement of these orbitals in $1a_1$ of ML_2. Since s-type orbitals have no intrinsic directional preference, a bond with large s admixture will point in the direction of least steric resistance. *Therefore, the group 3 metals, which have low-lying s orbitals, will prefer trigonal conformation more than the group 4 metals, for which the s orbitals are less accessible.* It should be pointed out that

Scheme 4

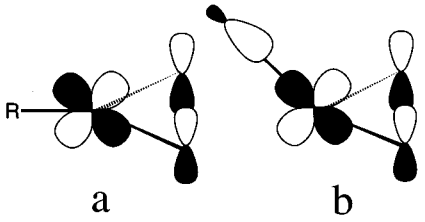

the $1a_1$, $2a_1$, and b_1 frontier orbitals of ML_2 have been discussed previously by Lauher and Hoffmann[56] in the case of L = Cp. However, it is clear from our study that the actual composition and relative spacing of these orbitals is highly dependent on L and the metal atom.

Figure 1 also shows that amido ligands have a stronger tendency toward trigonal conformation than hydroxy or methyl ligands. This can be rationalized in terms of π-bonding between the metal and ligand lone pairs as shown in Scheme 4. In the trigonal case (a), the lone pair orbitals on the ligands will interact with a nonbonding d orbital of relatively low energy. In the tetrahedral case (b), the lone pairs will interact with a d-orbital destabilized by interactions from the σ-orbitals of the R group, thus making the tetrahedral conformation more unfavorable. *Good π-donor ligands therefore have an increased tendency to form trigonal arrangements as opposed to weak π-donor ligands.*

The systematics derived above regarding the trigonal vs tetrahedral preference of $[L]MR^{n+}$ precursors agree well with previous calculations on [**4**]ScR[57] as well as Ti and Zr constrained-geometry catalysts.[58] They also pertain to systems with more realistic ligands done in the present paper. [**1**]ScC_2H_5(exo)[59] as well as [**1**]YC_2H_5(exo) are only stable in the trigonal conformation, whereas [**1**]$TiC_2H_5^+$(exo) is stable as well in trigonal and in tetrahedral conformation, the latter being less stable by 2 kJ/mol. Removing π-density from the nitrogen ligand by attaching a boron substituent results in a destabilization of the trigonal form in [**2**]$TiC_2H_5^+$(exo) by 13 kJ/mol relative to the tetrahedral form. The same holds for [**2**]ScC_2H_5(exo), for which the trigonal form is 1 kJ/mol less stable than the tetrahedral one. Following a general destabilization trend of the trigonal form down the triad, [**1**]$ZrC_2H_5^+$(exo) is less stable by 9 kJ/mol in the trigonal form than in the tetrahedral one. [**1**]LaC_2H_5(exo) is only stable in tetrahedral form, whereas the tetrahedral form is favored by 30 kJ/mol over the trigonal one for [**1**]$HfC_2H_5^+$(exo). Both [**1**]$ThC_2H_5^+$(exo) and [**1**]LuC_2H_5(exo) are only stable in tetrahedral form. Going from sterically relatively unencumbered ligands to bulky ones, we see that steric pressure around the central atom leads to increasing preference of the trigonal conformation. For the bis-Cp systems [**4**]ScC_2H_5, [**4**]$TiC_2H_5^+$, [**4**]$ZrC_2H_5^+$, and [**4**]$HfC_2H_5^+$, the transformation angle θ (Table 4) is close to 165,° which is nearly trigonal, although Hf exhibits a strong intrinsic

(56) Lauher, J. W.; Hoffmann, R. *J. Am. Chem. Soc.* **1976**, *98*, 1729.
(57) Ziegler, T.; Folga, E.; Berces, A. *J. Am. Chem. Soc.* **1993**, *115*, 636.
(58) Woo, T. K.; Fan, L.; Ziegler, T. *Organometallics* **1994**, *13*, 2252.
(59) Ligands **1** and **10** are puckered (i.e. they have C_s instead of C_{2v} symmetry) and therefore give rise to exo−endo isomerism with regard to the attached alkyl chain. If the alkyl chain terminus points toward the concave side of the ligand, it will be termed endo. If it points toward the convex side of the ligand, it will be termed exo.

Table 3. Dependence of Agostic Bond Strengths of $L_2MC_2H_5^{n+}$ on the Metal Center and Ligand[a]

	$\Delta E_{\beta-\text{agostic}}$[a]				$\Delta E_{\beta-\text{agostic}}$[a]		
metal	L = CH_3	L = NH_2	L = OH	metal	L = CH_3	L = NH_2	L = OH
Sc	7	7	6	Ti	11	13	19
Y	10	8	6	Zr	13	12	21
La	3	3	5	Hf	2	2	3
Lu[b]				Th	7	8	11

[a] In kJ/mol. $\Delta E_{\beta-\text{agostic}}$(M) equals the energy used to deform the optimized $L_2MC_2H_5^{n+}$ fragment into a geometry where all degrees of freedom were optimized except for the M−C_α−C_β angle which is constrained to 109.45°. At this angle, agostic bonds are destroyed. The L−M−L angle was constrained to 90°. [b] $L_2LuC_2H_5$ does not undergo agostic bonding.

aversion against trigonal coordination. *We can conclude from this that apart from the intrinsic preference of the metal for a given configuration, steric pressure modifies the potential surface in favor of the trigonal configuration.*

(1.b) Trends in Agostic Bond Strength with Respect to Variation of Metal and Auxiliary Ligand and Their Influence on the Preference for Trigonal vs Tetrahedral Conformation. To separate out the influence which agostic interactions might have on the preference for trigonal vs tetrahedral conformation, we performed a series of calculations for $L_2MC_2H_5^{n+}$ (M = Sc, Y, La, Lu, Ti, Zr, Hf, Th; L = CH_3, NH_2, OH), varying its structure from tetrahedral to trigonal (Figure 3[60]).

Figure 3 shows that the behavior noted for the methyl complexes also persists for β-agostically bonded ethyl complexes. The trigonal structure is only favored for $(NH_2)_2ScC_2H_5$, and a local trigonal minimum exists for $(NH_2)_2TiC_2H_5^+$. For all other metals, the trigonal conformation is unstable. However, the bias toward tetrahedral conformation is lessened for $L_2MC_2H_5^{n+}$ compared to $L_2MCH_3^{n+}$. *The β-agostic bond therefore only weakly perturbs a potential surface that is primarily modeled by the metal framework. It stabilizes the trigonal conformation more than the tetrahedral conformation.*

Despite playing such a crucial role in organometallic chemistry, agostic interactions are hard to quantify as they are not unambiguously separable from the entity of metal−alkyl bonding. Although hard to determine in absolute terms, it is easier to determine trends in agostic bond strengths within one group of metals. In all subsequent deliberations, agostic bond strengths will be discussed in strictly defined terms chosen to best deal with the problem at hand.

To quantify agostic bonding, we use a straightforward definition of β-agostic bond strength:

$$\Delta E_{\beta-\text{agostic}} = E[L_2MC_2H_5^{n+}] - E^*[L_2MC_2H_5^{n+}] \quad (1)$$

Here $E[L_2MC_2H_5^{n+}]$ refers to an energy determined for the ground state of the compound in which the β-agostic bond is present (Scheme 5a), whereas E^* corresponds to a total energy derived for a compound whose M−C_α−C_β angle is constrained to its ideal tetrahedral value of 109.45° (Scheme 5b). This additional constraint disrupts the β-agostic bond. The quantities measured thereby are mainly the rupture of covalent interactions between the β-C−H bond and metal and the strain energy that is released when the alkyl chain returns into its "natural", staggered conformation.

Scheme 5

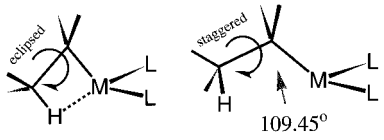

a b

Table 3 shows that according to this criterion, the agostic bond strengths *(a) are almost constant for the first two metals in a triad but diminish markedly for the heaviest element of the triad and (b) are generally stronger for charged species than for uncharged species (with the exception of La, for which the agostic bond is as strong as for Hf).* (a) has its origin in the fact that the agostic bond is stabilized by donation from the C−H σ orbital into empty metal d orbitals. As the metal d orbital energies of the $L_2MC_2H_5^{n+}$ fragment rise toward the bottom of the triad, this contribution and therefore agostic stabilization diminishes. (b) is due to loss of electrostatic attraction as one goes from charged group 4 complexes to neutral group 3 complexes and a concomitant increase of metal d orbital energies. Trends of agostic bond strength with respect to ligand variation are less clear-cut and do not follow an apparent trend that pertains to all metals.

(2) π-Complexation of C_2H_4 To Form $[L]MC_2H_5(C_2H_4)^{n+}$ (n = 0, 1, 2). (2.a) Decomposition of the Olefin Uptake Energy. Uptake of C_2H_4 by compounds of the type $[L]MC_2H_5^{n+}$ has been shown previously to result in a π-complex rather than an "end-on" complex whereby the hydrogen atoms coordinate in a chelating fashion to the metal.[28] The π-complexes formed show very little orientational preference of the olefin with respect to the rest of the catalyst. Generally, the rotational barriers for torsion about the metal−olefin bond are lower than 15 kJ/mol. This is in line with previous molecular dynamics calculations, which show that, for [**4**]$ZrC_2H_5(C_2H_4)^+$ [61] and [5]$TiC_3H_7(C_2H_4)^+$,[32] the olefin rotates freely at room temperature. We have calculated the structure and total energy of all olefin π-complexes listed in Table 4.

The total energy gain ΔE_{uptake} for the reaction $[L]MC_2H_5^{n+} + C_2H_4 \rightarrow [L]MC_2H_5(C_2H_4)^{n+}$ can be decomposed according to eq 2,[62−64] where ΔE_{def} refers to the

$$\Delta E_{\text{uptake}} = \Delta E_{\text{def}} + \Delta E_{\text{combination}} = \Delta E_{\text{def}} + \Delta E_{\text{Pauli}} + \Delta E_{\text{elstat}} + \Delta E_{\text{orbital}} + \Delta E_{\text{rel}} \quad (2)$$

energy required to deform the gas-phase optimized geometries of free $[L]MC_2H_5^{n+}$ and free C_2H_4 into the structures they assume in the product $[L]MC_2H_5(C_2H_4)^{n+}$. Further, $\Delta E_{\text{combination}}$, consisting of a Pauli

(60) These calculations were performed with the same set of constraints as was applied for the analogous methyl system. However, the movement of the β-carbon atom is restricted to the plane normal to the auxiliary ligand plane.

(61) Margl, P.; Lohrenz, J. C. W.; Ziegler, T.; Blöchl, P. E. *J. Am. Chem. Soc.* **1996**, *118*, 4434.

(62) Ziegler, T. In *NATO ASI Series C*; Salahub, D., Ed.; Kluwer: Dordrecht, The Netherlands, 1992; Vol. 378; p 367.

(63) Ziegler, T.; Rauk, A. *Inorg. Chem.* **1979**, *18*, 1755.

(64) Ziegler, T.; Rauk, A. *Theoret. Chim. Acta* **1977**, *46*, 1.

Table 4. Ethylene Complexation Energies and Related Data for All Compounds Investigated

metal	ligand	ΔE^a C_2H_4 uptake FS	ΔE^a C_2H_4 uptake BS	metal radius[b]	cryst ionic radius[b]	θ (precursor)	metal surface area[c]
Sc(III)	**1**-exo	−30	−45	1.59	1.383	168	35
	2-exo	−53	−45			133	34
	3	−85	−60			125	33
	4	0	−5			167	12
	7	−38	−47			178	38
	8	−46	−46			150	33
	9	−46	−41			140	39
Y(III)	**1**-exo[h]	−45	−52 [−52]	1.80	1.688	173	59
	7	−50	−48			165	62
	8	−53	−43			147	57
	9	−55	−40			143	65
La(III)	**1**-exo[h]	−38	−42 [−43]	1.91	1.92	146	82
	7	−36	−23			148	81
	8	−38	−21			142	78
	9	−40	−18			128	88
Lu(III)	**1**-exo	−58	*i*	1.75	1.606	132	57
Ti(IV)	**1**-exo	−88	−87	1.48	1.285	163	23
	1-endo	−74	−82			172	25
	2-exo	−90	−78			127	22
	2-endo	−74	−82			170	25
	3	−161	−			120	23
	4	−8	−13			165	4
	5[e]	−72	−75			175	14
	7	−96	−100			131	23
	8	−109	−94			117	22
	9	−102	−83			127	26
	10-exo[d]	−64	−80			162	19
	10-endo[d]	−70	−77			172	19
Zr(IV)	**1**-exo[h]	−97	−86 [−90]	1.64	1.493	124	39
	3	−165				121	38
	4[f]	−37	−44			168[j]	12
	7	−104	−97			137	40
	8	−109	−83			118	38
	9	−112	−83			129	43
	10-exo[d]	−88	−95			163	36
	10-endo[d]	−90	−92			172	35
Hf(IV)	**1**-exo[h]	−101	−101 [−101]	1.64	1.474	119	42
	4	−63	−63			167	15
	7	−87	*i*			114	43
	8	−101	*i*			113	42
	9	−86	*i*			109	48
	10-exo[d]	−85	−89			123	37
	10-endo[d]	−80	−68			124	41
Ce(IV)	**1**-exo[h]	−62	−49 [−50]	1.80	1.739	128	69
Th(IV)	**1**-exo	−74	*i*	1.80	1.927	116	66
V(V)	**6**	−29	−14	1.38	1.115	n/a	3
Nb(III)[g]	**1**-exo	−227	−207				

[a] In units of kJ/mol, calculated with respect to free C_2H_4 and the energetically most favorable isomer of the precursor $[L]MR^{n+}$. In case of exo−endo isomerism, energies are calculated with respect to precursor compounds of the same type so that exo (endo) complexation energies are given with respect to exo (endo) precursors. All compounds of Ti, Zr, Hf, Ce, Th, and V bear one positive charge except for compounds of ligand **3**, which bear two positive charges. All compounds of Sc, Y, La, Lu, and Nb are uncharged except for compounds of ligand **3**, which have one positive charge. [b] In units of Å. The relative size of "accessible surface" radii was determined by comparing the M−N bond lengths in $[\mathbf{1}]MC_2H_5^{n+}$. However, crystal ionic radii of the respective d^0 ions are correlated linearly with the radii used for construction of the accessible surface ($R = 0.965$). [c] In units of $bohr^2$. 1 $bohr^2 = 0.2800$ $Å^2$. [d] As calculated by Deng and Ziegler,[48] with the polymer chain modeled by a propyl group. [e] As calculated by Woo et al.[32] using BP86 energetics for LDA geometries. [f] Obtained by Lohrenz et al.[30] using BP86 energetics for LDA geometries. [g] This is a d^2 system and is shown for comparison only. [h] For some compounds of the type $[\mathbf{1}]MC_2H_5^{n+}$, BS(exo) and FS(endo) π-complexes lie energetically as well as spatially very close together. Due to the flatness of the potential energy surface with regard to this interconversion, we give in brackets the formation energy of the FS(endo) isomer with respect to the exo precursor. However, the geometries of these complexes are very floppy with regard to rotation about the metal−C_α bond, so that the BS(exo) and FS(endo) π-complexes are easily interchangeable for all metals heavier than Sc and Ti. [i] Does not form a stable BS π-complex due to lack of agostic bonding. [j] The structure by Lohrenz et al.[30] derived from LDA calculations had a θ value of 143°. Re-optimization at the nonlocal level yielded 168°.

repulsion, an electrostatic, and an orbital interaction term, is the energy gained by combining the deformed fragments together to form the product $[L]MC_2H_5(C_2H_4)^{n+}$.

The Pauli term, ΔE_{Pauli}, represents the four electron two orbital repulsive interaction between occupied orbitals. It can also be identified with the steric interaction energy between the two fragments. The

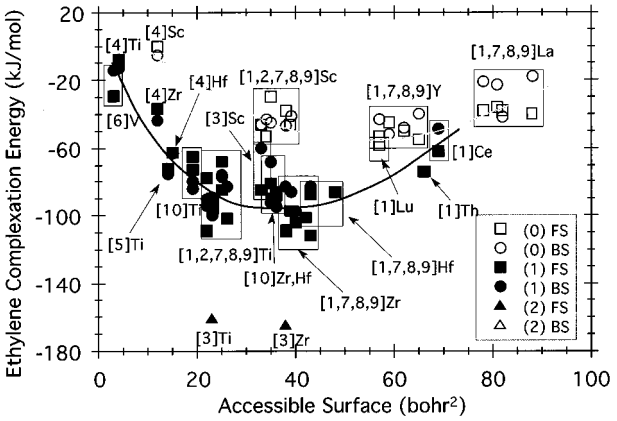

Figure 4. Ethylene complexation energy (kJ/mol) vs accessible surface of the metal (bohr²). Rectangles refer to FS complexation energies, whereas circles show BS complexation energies. Filled rectangles and circles refer to singly charged species. Doubly charged systems are shown indicated by triangles. [**3**]Ti and [**3**]Zr, shown by triangles, form stable FS complexes only.

contribution $\Delta E_{orbital}$ stems from the stabilizing interaction between occupied and virtual orbitals on the [L]-$MC_2H_5^{n+}$ and C_2H_4 fragments and is often identified with the "electronic" contribution to the bonding energy. The electrostatic interaction between the charge distributions (nuclear charge and electron density) of the two fragments is represented by ΔE_{elstat}. The relativistic contribution to the binding energy is given by ΔE_{rel}.

(2.b) Effect of Total Charge on the Metal Fragment. The calculated π-complexation energies are in a very straightforward manner related to the total charge of the catalyst complex. As Table 4 shows, doubly charged species ([**3**]$TiC_2H_5^{2+}$ and [**3**]$ZrC_2H_5^{2+}$) bind ethylene in a strongly exothermic reaction ($\Delta E_{uptake} \approx -160-170$ kJ/mol), whereas singly charged species show much smaller π-complexation energies (exothermic up to ≈110 kJ/mol, depending on steric constriction of the site). Neutral species show the smallest adduct formation energies (exothermic up to ≈60 kJ/mol).

The term responsible for the influence of the total charge on the complexation energy is the electrostatic term ΔE_{elstat}. This term is in general stabilizing for the systems at hand. For the neutral systems the largest contribution to ΔE_{elstat} comes from the penetration of the density cloud of the π-electron pair on ethylene into the electron density of the metal fragment. The penetration makes the shielding of the nuclei on the metal fragment by its electrons incomplete, leading to a net electrostatic attraction between the π-electron pair and the metal fragment. The electrostatic attraction between the π-electron pair and the metal fragment will be enhanced further as the total positive charge on the latter increases (Table 4 and Figure 4). The importance of the electrostatic contribution in d^0 metal−olefin binding is contrasted nicely by the example of a d^2 system ([**1**]NbC_2H_5), which binds ethylene in covalent fashion by donation of two metal d electrons into the olefin π^* orbital. Correspondingly, olefin uptake is approximately three times as exothermic as for neutral group 3 species (Table 4).

(2.c) Effect of Steric Constriction around the Metal Center. Figure 4 and Table 4 show that there is a distinct relationship between the accessibility[65] of the metal and π-complex formation energy. Between 0 and ≈30 bohr² of accessible surface on the metal ion, the ethylene binding energy becomes stronger almost linearly as the accessible surface increases. This can be rationalized as follows: the openness of the metal site is important in presenting entrance channels and binding sites to the incoming olefin. Therefore, a sterically constricted site will be less likely to form a π-complex, since (i) no entrance channels are open a priori and (ii) an entrance channel can only be opened by predissociation of the agostic bond. As an objective measure of steric constriction, one may take the accessible surface area of the metal atom. By calculating the accessible surface area of a Ti atom complexed with various ligands, we can order our systems according to rising accessibility as **4** < **5** < **10** ≤ **8** ≈ **7** ≈ **1** ≈ **2** ≈ **3** ≤ **9**. Correspondingly, we find the same ordering of π adduct formation energies: $\Delta E_{uptake} \approx -10$ kJ/mol (bis-Cp, **4**), and −75 kJ/mol (mono-Cp, **5**) and $\Delta E_{uptake} \approx -100$ kJ/mol for sterically unhindered systems. For doubly charged systems ([**3**]$TiC_2H_5^{2+}$ and [**3**]$ZrC_2H_5^{2+}$), adduct formation is much more exothermic due to a large electrostatic binding contribution. For group 3 neutrals such as Sc, on the other hand, a sterically demanding ligand such as **4** effectively prohibits formation of a stable π-complex ([**4**]ScC_2H_5, Table 4), whereas sterically unhindered ligands allow uptake energies of ≈−45 kJ/mol. Analogous to Ti, adduct formation of the singly charged species [**3**]$ScC_2H_5^+$ is much favored ($\Delta E_{uptake} = -60$ to −85 kJ/mol) over uncharged species due to the charge effect (+1 for **3** as opposed to 0 for all other ligands).

Figure 4 also shows that the uptake energies eventually rise beyond an accessible surface of ≈50 bohr², where mostly lanthanide and actinide ions reside. We attribute this (a) to the decay of electrostatic penetration energy ΔE_{elstat} as the radius of the metal increases and the ethylene moiety is removed from the charge cloud of the catalyst and (b) to a rise of metal d orbital energies as they become more diffuse. *Although the empirical relationship shown in Figure 4 allows a good guess of the olefin uptake energy once the accessible surface area on the metal is known, the correlations between energy and accessible area at the metal ion are clearly not reliable enough to make a prediction with less than 20 kJ/mol error.* The residual spread observed in Figure 4 stems mainly from the fact that FS and BS complexation energies can be greatly different for one and the same metal. This effect can be traced back to Figure 3 and is a function of the metal and the ligand that manifests itself in the deformation contribution to the uptake energy (ΔE_{def}). Furthermore, steric effects might not necessarily manifest themselves in the ac-

(65) "Accessibility" here is measured by the surface area of the metal open to ethylene coordination. It is determined by surrounding each atom of the molecule with a sphere of a given radius (see below) and, after discarding those parts of the sphere that lie within another atomic sphere, measuring the surface area associated with this atom. The following atomic radii were used (in bohr units): $R_H = 2.07$, $R_C = 3.3$, $R_N = 3.2$, $R_O = 3.27$, $R_B = 3.0$; for metals, V(V) 2.6, Ti(IV) 2.8, Sc(III) 3.0, Zr(IV) 3.1, Hf(IV) 3.1, Lu(III) 3.3, Y(III) 3.4, Ce(IV) 3.4, Th(IV) 3.4, La(III) 3.6. This choice of atomic radii is derived from electrostatic solvation models used in our group which are devised to model the accumulation of electric charge due to surrounding solvent. They are chosen to reflect the molecular surface accessible to a small solvent molecule. For metal atoms, radii were chosen that resulted in a good linear relationship with the corresponding crystal ionic radii (Table 4).[68]

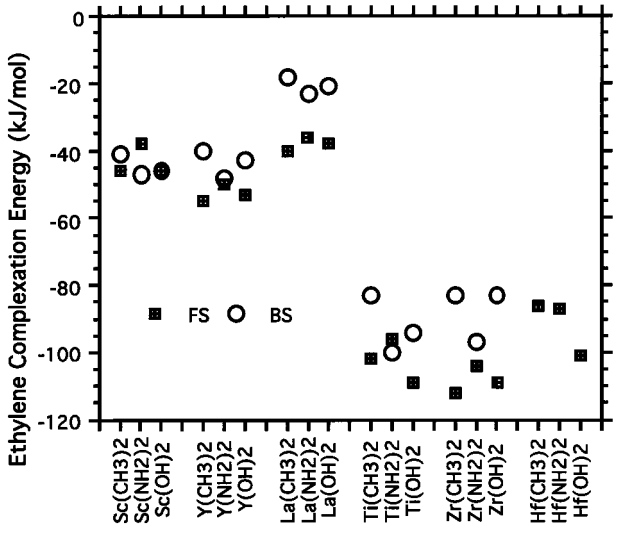

Figure 5. Ethylene complexation energetics (kJ/mol) of sterically minimal systems [**7**−**9**]$MC_2H_5^{0,+}$. *x*-axis labels do not include the ethyl group and total charge. [**7**−**9**]$HfC_2H_5^+$ do not form stable BS complexes.

cessible surface area but still restrict the conformational freedom so much that the uptake energy is affected. A good example of this is [**10**]$HfC_3H_7^+$, where exo−endo isomerism of the precursor alone influences the uptake energy by 22 kJ/mol. Moreover, the difference between FS and BS complexation induced by configurational preference (trigonal vs tetrahedral) of the precursor is 13 kJ/mol for [**10**]$HfC_3H_7^+$(endo).[48] Since those effects can be additive, it appears hardly possible to predict olefin uptake energetics to an accuracy of better than ±20 kJ/mol from empirical lookup charts such as shown in Figure 4. Furthermore, the accessible surface area does not reliably reflect trends in uptake energies if there is little or no steric congestion: the complexes [**7**]-$MC_2H_5^+$ (M=Ti, Zr, Hf) all show very similar ethylene π-complexation energies although their accessible surface areas are quite different. To explain this, one must account for the different electronic makeup of the metal.

(2.d) Electronic Factors of Importance for the Ethylene Uptake Energy. The relatively large residual spread of olefin uptake energetics apparent from Figure 4 needs to be explained. To separate the responsible factors into such introduced by steric factors not included in the accessible area and such which are due to the electronic makeup of the metal and the coordinating atoms, a series of calculations was done whereby various metals (Sc, Y, La, Ti, Zr, Hf) were ligated by CH_3, NH_2, or OH groups, respectively. A constraint was put on the L−M−L angle to keep the ligands at a typical bidentate angle of 90° to each other. We will assume that as a first approximation there is no steric hindrance from such small ligands, and therefore trends observed for π-complexation to such compounds will only reflect changes of properties related to the electronic makeup of metal and ligands. However, some steric repulsion still remains due to the occupied orbitals of $L_2MC_2H_5^{n+}$, which will be considered negligible in the following discussion.

(2.d.1) Front-Side vs Backside Complexation. As shown in Figure 5, most sterically minimal (minimal in the sense of having the least steric constriction) systems show a decisive preference of FS over BS coordination, whereas only a few prefer BS over FS coordination ($(NH_2)_2TiC_2H_5^+$ and $(NH_2)_2ScC_2H_5$, which are the only ones which have stable trigonal precursor fragments; see Figure 3). In the following we show that the preference of BS or FS, respectively, changes systematically as one goes from Sc to La and from Ti to Hf. This is due to a preference of the precursor complex $L_2MC_2H_5^{n+}$ to be either in a trigonal or tetrahedral conformation, since the structure of the precursor fragment in the BS π-complex is very close to trigonal, whereas the structure of the precursor in the FS π-complex resembles a tetrahedral configuration. Depending on the preference of the $L_2MC_2H_5^{n+}$ fragment to be tetrahedral or trigonal either BS or FS complexation is favored. *The BS π complex will be favored over the FS π complex only if the precursor fragment $L_2MC_2H_5^{n+}$ is stable in a trigonal conformation or the energy difference between trigonal and tetrahedral is small.*

(2.d.2) Variation with Respect to the Metal. Taking an average uptake energy that is the mean of FS and BS uptake energies shown in Figure 5, one finds the following trend: uptake energies are more exothermic for second-row transition metals than for first-row transition metals. For third-row transition metals, uptake is least exothermic. To find out why, we have broken down the FS and BS uptake energies for compounds of the type $(NH_2)_2MC_2H_5^{n+}$ (M = Sc, Y, La, Ti, Zr, Hf). Lu and Th were omitted since their relationship to the other metals is rather blurred, thus rendering systematic comparisons cumbersome. $(NH_2)_2$ was chosen as a ligand because it exhibits the smallest bias toward either BS or FS complexation. It is assumed that all following arguments based on those calculations are also valid for OH and CH_3 ligands.

From Table 5 we can conclude that with minimal steric factors, olefin uptake energies for metals are determined by a few simple trends: *(a) In terms of absolute size, ΔE_{uptake} is smallest for the heaviest metal in the triads and largest for the 4d metals.* This is primarily accounted for by $\Delta E_{orbital}$, which is markedly smaller for third-row metals than for first- and second-row metals. We attribute this to a rise of the metal d acceptor orbitals as one goes from Sc to La and from Ti to Hf, as is mirrored in the LUMO single particle energies for the precursor compounds $L_2MC_2H_5^{n+}$ (Table 5). For the Sc triad, this trend is enforced by a loss of electrostatic penetration energy as the size of the metal increases (especially for La) as shown by ΔE_{elstat}. Whereas Zr and Hf stay relatively compact compared to Ti, ionic radii rise much stronger in the Sc triad since there is no lanthanide contraction. This trend is much less pronounced for the Ti triad, where the lanthanide contraction causes Hf to be only marginally bigger than Zr. *(b) FS complexation is increasingly facilitated by a diminishing deformation energy down the triads, due to a increasing preference for the tetrahedral conformation.*[66] *From the decreasing preference for trigonal conformation follows that BS complexation is more facile for light metals than for heavy metals.*

(66) An exception is $[L]HfC_2H_5^+$, for which the deformation energy is misleadingly large since there is no agostic bond present in the precursor but one is formed upon FS olefin complexation. Thus, the large deformation incurred on complexation overcompensates the contribution from tetrahedral−trigonal isomerism.

Table 5. FS and BS Ethylene π-Complexation Energetics of $(NH_2)_2MC_2H_5^{n+}$ [a]

	ΔE_{Pauli}	ΔE_{elstat}	ΔE_{steric}	$\Delta E_{orbital}$	ΔE_{combi}	ΔE_{def}	ΔE_{rel}[b]	ΔE_{uptake}[c]	E_{LUMO}[d]
				FS					
Sc	134	−115	21	−71	−52	15	0	−38	−203
Y	114	−102	12	−63	−51	4	−2	−50	−202
La	84	−78	6	−44	−38	2	(−6)	−36	−185
Ti	171	−149	22	−124	−103	8	−2	−96	−833
Zr	167	−147	20	−122	−102	4	−4	−104	−770
Hf	169	−151	18	−117	−98	12	(3)	−87	−736
				BS					
Sc	155	−128	27	−79	−53	5	0	−47	−203
Y	156	−126	30	−83	−54	7	−2	−48	−202
La	59	−60	−1	−29	−31	8	(−3)	−23	−185
Ti	184	−161	23	−131	−107	8	0	−100	−833
Zr	197	−165	32	−137	−105	11	−3	−97	−770
Hf[e]									

[a] $\Delta E_{Pauli} + \Delta E_{elstat} = \Delta E_{steric}$. [b] Values in parentheses are relativistic corrections which are already contained in ΔE_{combi} and ΔE_{def}. [c] Individual contributions might not exactly add up to ΔE_{uptake} due to roundoff errors. [d] E_{LUMO} refers to the LUMO orbital energy in the precursor fragment $(NH_2)_2MC_2H_5^{n+}$. [e] $(NH_2)_2HfC_2H_5^+$ does not form a stable BS π-complex due to lack of agostic bonding.

Table 6. FS and BS Uptake Energy for $L_2TiC_2H_5^+$, Where L = CH_3, NH_2, and OH[a]

	ΔE_{Pauli}	ΔE_{elstat}	ΔE_{steric}	$\Delta E_{orbital}$	ΔE_{combi}	ΔE_{def}	ΔE_{rel}	ΔE_{uptake}[b]	E_{LUMO}[c]
				FS					
$(CH_3)_2$	183	−150	33	−140	−108	8	−2	−102	−863
$(NH_2)_2$	171	−149	22	−124	−103	8	−2	−96	−833
$(OH)_2$	180	−157	23	−140	−116	8	−1	−109	−877
				BS					
$(CH_3)_2$	224	−175	49	−166	−117	33	0	−83	−863
$(NH_2)_2$	184	−161	23	−131	−107	8	0	−100	−833
$(OH)_2$	212	−177	35	−162	−127	33	0	−94	−877

[a] $\Delta E_{Pauli} + \Delta E_{elstat} = \Delta E_{steric}$. [b] Individual contributions might not exactly add up to ΔE_{uptake} due to roundoff errors. [b] E_{LUMO} refers to the LUMO orbital energy in the precursor fragment $L_2TiC_2H_5^{n+}$.

(2.d.3) Variation with Respect to the Ligand. Making use of the same decomposition technique as above, we now turn to the variations of uptake energy with respect to the ligand, using complexes of the type $[L]TiC_2H_5^+$ (L = $(CH_3)_2$, $(NH_2)_2$, $(OH)_2$) as a model.

The results of those calculations (Table 6) show that the $(NH_2)_2$ ligand set prefers BS uptake, whereas the $(CH_3)_2$ and $(OH)_2$ ligand sets prefer FS uptake. This result can be rationalized solely by considering two factors that influence the binding energy, namely the deformation energy contribution ΔE_{def} and the orbital interaction contribution $\Delta E_{orbital}$. (a) $(NH_2)_2TiC_2H_5^+$ needs only 5 kJ/mol to execute a conformational change from tetrahedral to trigonal, whereas $(OH)_2TiC_2H_5^+$ and $(CH_3)_2TiC_2H_5^+$ need 25 and 40 kJ/mol, respectively, to achieve the same change (Figure 3). Therefore, replacing the amido ligand set by a methyl or hydroxyl ligand set drastically alters the preference toward tetrahedral coordination and, thus, FS π-complexation. (b) The contribution of orbital interactions $\Delta E_{orbital}$ to the binding energy is smaller for $(NH_2)_2TiC_2H_5^+$ than for the methyl and hydroxy system on the other hand, due to a LUMO which is destabilized by π-interactions with the auxiliary ligands (LUMO energies are given in Table 6; for schematics see Scheme 4). This effect pertains to both FS and BS complexation to an amido system, but for BS complexation this feature is overcompensated by a favorably small deformation energy ΔE_{def}. *We conclude that since an amido ligand—relative to an alkyl or hydroxy ligand—more strongly prefers the trigonal conformation, BS uptake is favored over FS uptake for amido-coordinated systems. Since $(CH_3)_2$ and $(OH)_2$ ligands more strongly prefer a tetrahedral arrangement of ligands, FS uptake is favored for them. Because the conformational preference for tetrahedral or trigonal is mutually exclusive, FS and BS complexation energies always show an exactly mirror symmetric trend.* Although this rule is derived considering complexes of Ti only, Figure 5 shows that this mirror symmetric pattern holds true for all group 3 and group 4 metals. This confirms that a large part of the residual spread of uptake energies in Figure 4 which is not taken into account by accessible surface considerations is due to an intrinsic preference of the given metal−ligand combination toward either trigonal or tetrahedral configuration.

(2.e) Trends in the Uptake Energies for Realistic Ligand Systems. If a more realistic auxiliary ligand is coordinated to the metal, steric factors modify the potential surface of olefin uptake as described in section 2.c. As shown in Figure 4, steric influences (ΔE_{Pauli}) mainly act through modifications of the accessible surface of the metal. However, not all steric changes might manifest themselves in that quantity. Ligands **1** and **10**, for instance, restrict the angular freedom of the alkyl chain without a noticeable decrease of the accessible surface compared to the sterically minimal ligand **7**. Therefore it is necessary to show how these additional factors affect olefin complexation energetics. However, since calculations for realistic systems are much more time-consuming than for minimal systems, we will limit our analysis to systems with auxiliary ligands **1**, **4**, and **10**.

In Figure 6 we juxtapose π-complexation energies for [**4**]$MC_2H_5^{n+}$ and various isomers of [**1**]$MC_2H_5^{n+}$ and [**10**]-$MC_2H_5^+$.

$(Cp)_2MC_2H_5^{n+}$. Starting with the sterically most hindered ligand **4**, it becomes immediately obvious that the uptake energies are strongly determined by the available space around the metal ion. The larger the

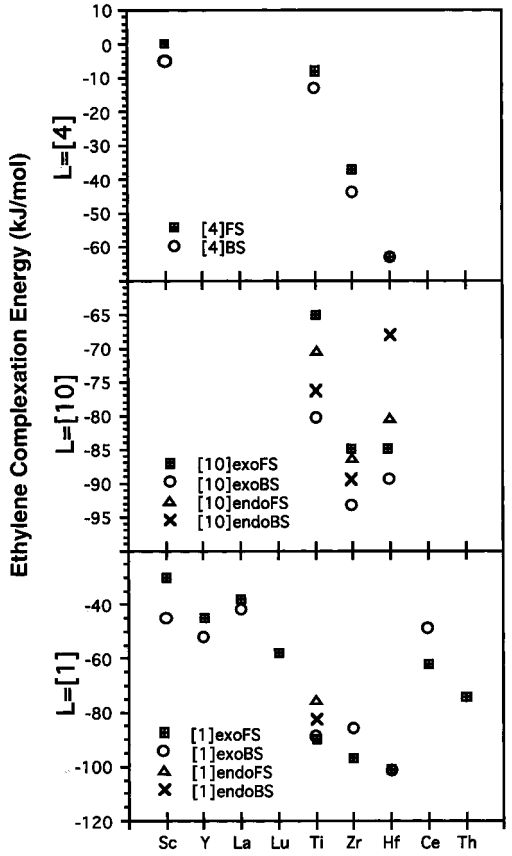

Figure 6. Ethylene complexation energetics (kJ/mol) for realistic systems [**4**]$MC_2H_5^{0,+}$, [**10**]$MC_3H_7^+$, and [**1**]$MC_2H_5^{0,+}$. The Sc, Y, La, and Lu systems are neutral. The Ti, Zr, Hf, Ce, and Th systems bear one positive charge. Calculations for ligand **10** are taken from Deng et al.[48]

ion gets, the more the site is opened and the more exothermic the complexation process becomes. Whereas Ti forms only a weak electrostatic adduct with ethylene, Hf forms a full-fledged close-contact π-complex with a concomitant increase in binding energy. Due to steric crowding, all Cp systems have a θ angle of around 165°, although calculations on smaller systems show that the conformational preference is highly dependent on the metal (Figure 5). BS coordination is preferred since the steric congestion favors a more trigonal arrangement of the precursor. Also, the [**4**]M fragment has C_{2v} pseudosymmetry, which reduces the number of possible isomers and thereby the spread of uptake energies. Thus for **4**, the relative stability of the π-complex is dominated by the accessible surface and the residual spread not accounted for by accessibility criteria is negligible, so the observed π-complexation energies can be explained satisfactorily by the systematics derived above.

[10]$MC_3H_7^{1+}$. Ligands **1** and **10** on the other hand are sterically relatively unencumbered but have low symmetry. From the viewpoint of accessibility and charge they are almost identical with **7**. They are however different from **7** in that they have additional isomers due to exo−endo isomerism.[59] Also, ligand **1** has a double bond that can donate electrons to the metal center. As becomes apparent from Figure 6, this gives rise to great variability of π-complexation energies. Ligand **10** leaves a slightly smaller surface area at the metal than ligand **7**; also there is some additional steric encumbrance from the propyl group (instead of an ethyl group that was used for **7**) which does not show up in the accessible surface area, so that the observed complexation energies are smaller for **10** than for **7**. This is especially the case for the smallest metal in the triad (Ti), for which the complexation energies are decreased in absolute size compared to the other metals. Also, the ring puckering exhibited by **10** (which is of C_s rather than C_{2v} symmetry) imposes some restrictions upon the openness of the site that do not enter into the accessible surface area (since this effect is exerted by the remote part of the ligand which does not touch the sphere of the metal). The more asymmetric the ligand system is, the more difficult it is to predict the resulting spread of complexation energies, since a departure from C_{2v} symmetry blurs the distinction between FS and BS isomers and creates new possibilities for ligand arrangement. The relative energies of the isomers created thus can, unfortunately, not be accounted for in simple terms, since they are determined by the precise makeup of the auxiliary ligand. Apart from that, these additional factors might alter the overall trends of the olefin complexation energy with respect to variation of the metal: a comparison of Figures 5 and 6 shows that complexes of ligand **7** ($-\Delta E_{\text{uptake}}$: Hf < Ti < Zr) show a different ordering than complexes of ligand **10** ($-\Delta E_{\text{uptake}}$: Ti < Hf < Zr). A further remarkable fact is that the amido groups in ligand **10** are held in completely planar position and so stabilize the trigonal conformation at the metal center even more so than ligand **7** (see θ values in Table 4), in which the amido groups have rotational freedom. Therefore, a trigonal arrangement around the metal center is even more favored than for **7**, which in turn shifts the preference toward BS π-complexation (Table 4).

[1]$MC_2H_5^+$. Except for Ti, only isomers of the exo type were considered in our calculations on ligand **1**. The situation here is analogous to that for ligand **10**, with the additional complication that **1** has a C=C double bond that donates electrons to the metal center. In terms of accessible area, [**7**]$MC_2H_5^{n+}$ is identical with [**1**]$MC_2H_5^{n+}$ so that the π-complexation energies are of very similar magnitude. The relative ordering of complexation energies for FS and BS isomers as well as with respect to the metal differs from systems of ligand **7**. For ligand **1**, Sc triad metals always prefer BS coordination, whereas, for ligand **7**, only Sc shows this characteristic. The same problem appears here as for [**10**]-$MC_3H_7^+$, namely that the departure from C_{2v} symmetry by ring puckering introduces new factors which defy all attempts at simple explanation. Lanthanides and actinides (Ce, Th, and Lu) show very similar uptake energies, around -70 ± 10 kJ/mol, despite the fact that the Ce and Th systems are positively charged and the Lu system is uncharged. The reason for this is that the Lu(III) ion is relatively compact and thus has a favorable contribution to bonding coming from ΔE_{elstat} and $\Delta E_{\text{orbital}}$, whereas the Ce(IV) and Th(IV) ions are large and have diffuse d orbitals since they are at the beginning of the lanthanide and actinide series, respectively. Thus their electrostatic and orbital contributions to π-bonding are comparatively weak.

We must conclude this section by stating that *important differences between sterically minimal and realistic ligand systems are caused by subtle steric effects that*

Scheme 6

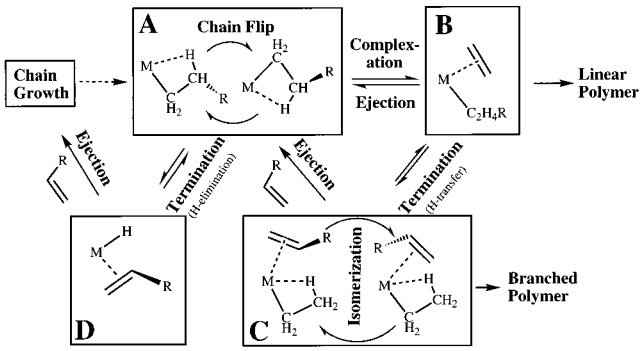

are impossible to quantify within any simple theory. It seems possible to predict the olefin complexation energy of d^0 and d^0f^n transition metal complexes to within ±20 kJ/mol by calculating the accessible surface on the metal and relating it to the graph in Figure 4, but detailed first-principles calculations have to be carried out to further improve this estimate.

(3) Influence of the Complexation Energy upon Polymerization Performance. (3.a) Activity and Molecular Weight. Olefin uptake energies calculated in the present work are widely spread and range from highly exothermic ($-\Delta E_{\text{uptake}} > 100$ kJ/mol) to thermoneutral. Taking into account an always unfavorable[67] uptake entropy, precursors $[L]MC_2H_5^{n+}$ for which $-\Delta E_{\text{uptake}}$ is smaller than 40−50 kJ/mol will not form a π-complex. Among the compounds investigated here, this will be the case for many uncharged and/or sterically hindered singly charged complexes (Figure 4 and Table 4). Thus, no precursor for insertion (Scheme 6B) is formed, giving rise to a negligible polymerization activity although the following insertion/propagation step itself might be very facile. We predict this to be the case for the bis-Cp Sc and Ti systems studied here since those have very small complexation energies. Not only activity can be detrimentally affected but also polymer molecular weight if π-complexation is so unfavorable as to allow competing termination mechanisms such as β-hydride elimination (Scheme 6D) to become effective. β-Hydrogen elimination can only take place if there is no monomer coordinated to the metal and thus will be faster if the population of the metal−alkyl precursor (Scheme 6A) is large compared to the π-complex (Scheme 6B). In light of our findings, one would expect that bis-Cp Ti systems are inferior polymerization catalysts compared to their Zr analogues: due to the difference of π-complexation energies of roughly 30 kJ/mol, the Zr π-complex population will be ≈170 000 times larger (at 300 K) than the population of the Ti π-complex under identical conditions. Lacking a precursor for insertion, the Ti catalyst will therefore be ineffective compared to the Zr catalyst both in terms of activity and chain length.

(3.b) Isomerization. Termination by hydrogen transfer to the monomer can be followed by either rotation of the chain or chain ejection. If the olefin π-complex is strong (such as for sterically unhindered, charged species), ejection of the vinyl terminated chain (Scheme 6; C → A) will be a slow process. Therefore, it is possible that the terminated chain will be reinserted before it can be ejected. The vinyl-terminated chain may rotate around the metal−olefin bond (Scheme 6C), giving rise to a branched polymer upon reinsertion. From our calculations it appears that such rotations of the chain are likely to be very fast at room temperature[32,61] due to small rotational barriers (usually below 15 kJ/mol). Uncharged or sterically hindered systems will likely eject the polymer chain once it is terminated. Thus, sterically unhindered, charged catalysts with very exothermic olefin complexation energies will tend to produce a longer polymer which is to some degree isomerized, whereas sterically hindered and/or uncharged catalysts will produce shorter, straighter polymer chains.

(3.c) Stereocontrol. Syndiotacticity control in polypropylene production hinges on a well-defined mode of attack of propylene on the metal−C_α bond, whereby the chain "swings" from one tetrahedral position into the opposite one, thus allowing insertions to take place in a strictly alternating fashion.[29] Two conditions can facilitate loss of stereocontrol: in case the β-agostic bond that anchors the polymer is weak (as for group 3 metals as well as Hf and Th; see Table 3), rupture of the β-agostic bond might allow for rotation about the M−C_α bond, so that stereocontrol is lost by chain flipping (Scheme 6A). An additional necessary condition for rapid chain flipping is that the barrier for a change between tetrahedral and trigonal is small, since a successful flip can only be executed if the system can pass through the trigonal conformation. For light metals, for group 3 metals as well as for good π-donor ligands (especially amido ligands), the trigonal conformation is relatively favorable and so stereocontrol can potentially be lost.

Concluding Remarks

We have presented a systematic survey of the ethylene complexation process for several d^0 and d^0f^n transition metal compounds (M = Sc(III), Y(III), La(III), Lu(III), Ti(IV), Zr(IV), Hf(IV), Th(IV), and V(V)). A number of ligands (L = $NH(CH_2)_2NH^{2-}$ (**1**), $N(BH_2)(CH_2)_2(BH_2)N^{2-}$ (**2**), $O(CH_2)_3O^-$ (**3**), Cp_2^{2-} (**4**), $NHSi(H_2)C_5H_4^{2-}$ (**5**), $[(O)(O(CH_2)_3O)]^{3-}$ (**6**), $(NH_2)_2$ (**7**), $(OH_2)_2$ (**8**), $(CH_3)_2^{2-}$ (**9**), and $NH(CH_2)_3NH^{2-}$ (**10**)) has been attached to these metal centers to elucidate the influence of different ligand−metal combinations upon olefin π-complexation energies. It has been shown that the complexation energy of an ethylene molecule to a $[L]MC_2H_5^{n+}$ precursor can be predicted within ±20 kJ/mol by simple empirical rules, based on the accessible metal surface of the $[L]MC_2H_5^{n+}$ fragment and its gross charge. Olefin π-complexation energetics are subtly influenced by steric characteristics of the auxiliary ligand so that they are hard to predict beyond an

(67) (a) Although there are little experimental data available, existing evidence[67b] suggests that the $-T\Delta S$ contribution to the free energy of ethylene complexation for early transition metal d^0 compounds[67c] is identical to the 40−50 kJ/mol one observed at 300 K for late transition metal (Ni and Pd) d^8 compounds.[67d,e] At the present level of computational technology it is not practicable to give detailed estimates of the $T\Delta S$ contribution to ethylene binding based on *ab initio* calculations for such a large sample as ours. Therefore, we will assume that previously measured or calculated $T\Delta S$ contributions are transferable. (b) Rix, F. C.; Brookhart, M.; White, P. S. *J. Am. Chem. Soc.* **1996**, *118*, 8, 4746. (c) Woo, T. Unpublished result of $-T\Delta S = 42$ kJ/mol at 298 K obtained for [**5**]$TiC_2H_5^+ + C_2H_4$. (d) Musaev, D. G.; Froese, R. D. J.; Svensson, M.; Morokuma, K. *J. Am. Chem. Soc.* **1997**, *119*, 367. (e) Moscardi, G.; Woo, T. Unpublished result of $-T\Delta S = 50$ kJ/mol obtained for $(CH)_2(NH)_2NiC_3H_7(C_2H_4)^+ + C_2H_4$.

accuracy of ±20 kJ/mol without detailed first-principles calculations. The complexation energy will also have an impact on activity and polymer chain length: if no π-complex is formed due to a small complexation energy, activity will be small and, moreover, other (usually unfavorable) termination processes such as β-hydrogen elimination might eventually take over and detrimentally affect the polymer molecular weight. We predict this to be the case for scandocene and titanocene, which show the smallest complexation energies. The conformation of the π-complex (FS vs BS) is primarily determined by the nature of the metal ion: the aptitude to form a frontside π-complex increases as one moves down the triad and from group 3 metals to group 4 metals. Good π-donor ligands as well as sterically bulky ligands which restrain the mobility of the θ angle[69] enhance the aptitude toward BS complexation. The reason for this is an increasing preference for the tetrahedral configuration of the precursor fragment $[L]MC_2H_5^{n+}$ along these coordinates. In this context, it is interesting to note that β-agostic interactions only weakly modify a conformational preference (tetrahedral vs trigonal) that is primarily determined by the makeup of the metal–ligand framework. Agostic interactions of the $[L]MC_2H_5^{n+}$ precursors are shown to decrease in strength in the order Ti ≈ Zr > Th > Hf for $[L]MC_2H_5^{+}$ and Sc ≈ Y ≥ La > Lu for $[L]MC_2H_5$ for L = **7**–**9**, with agostic interactions for uncharged precursor complexes $[L]MC_2H_5$ generally being weaker than for charged precursor complexes. In case the β-agostic bond that anchors the polymer is weak (as for group 3 metals as well as for 5d, lanthanide, and actinide metals), the chain might flip by 180° rotations about the $M-C_\alpha$ bond, thus giving rise to loss of stereocontrol. This will especially happen in cases where the $[L]MR^{n+}$ precursor prefers the trigonal conformation and/or the barrier for a change between trigonal and tetrahedral is small, as it is for light metals and for group 3 metals as well as for good π-donor ligands such as amido groups.

Acknowledgment. This work has been supported by the Natural Sciences and Engineering Research Council of Canada (NSERC), as well as by the donors of the Petroleum Research Fund, administered by the American Chemical Society (ACS-PRF No 31205-AC3). P.M. acknowledges fruitful discussions with T. K. Woo.

Supporting Information Available: A listing of Cartesian coordinates (51 pages). Ordering information is given on any current masthead page.

OM9707578

(68) *CRC Handbook of Chemistry and Physics*, 60 ed.; Weast, R. C., Ed.; CRC Press, Inc.: Boca Raton, 1980.

(69) Deng, L.; Woo, T.; Ziegler, T.; Margl, P.; Fan, L. Submitted for publication in J. Am. Chem. Soc. A detailed study of steric factors in ethylene polymerization with McConville's diamido catalyst.[10,11]